

# An electron impact cross section set for CHF<sub>3</sub>

Mark J. Kushner<sup>a)</sup> and Da Zhang<sup>b)</sup>

University of Illinois, 1406 West Green Street, Urbana, Illinois 61801

(Received 4 January 2000; accepted for publication 21 June 2000)

Trifluoromethane, CHF<sub>3</sub>, is used for plasma etching of silicon compounds for microelectronics fabrication, and so there is interest in developing computer models for plasmas sustained in CHF<sub>3</sub>. Recent measurements of electron swarm parameters, and electron impact dissociation and ionization cross sections, have provided a sufficient basis to develop a working electron impact cross section set for CHF<sub>3</sub>. Such a cross section set is reported here. We found that increased energy losses from dissociative electronic excitation processes were required to reproduce experimental ionization coefficients. The cross sections for attachment are small with there being some uncertainty in their magnitude at low energies. The cross sections were used in a plasma equipment model for an inductively coupled plasma reactor and compared to discharges sustained in C<sub>2</sub>F<sub>6</sub>. For otherwise identical operating conditions, plasmas sustained in CHF<sub>3</sub> had higher electron and lower negative ion densities. © 2000 American Institute of Physics. [S0021-8979(00)02119-8]

## I. INTRODUCTION

Trifluoromethane, CHF<sub>3</sub>, is a gas extensively used in the microelectronics industry for etching of silicon compounds.<sup>1-3</sup> As a result, there is great interest in developing reaction mechanisms for gas mixtures containing CHF<sub>3</sub> for use in computer models of plasma processing reactors. Recent reviews and assessments of fundamental data<sup>4,5</sup> and recent measurements of electron swarm data in CHF<sub>3</sub><sup>6</sup> and Ar/CHF<sub>3</sub> mixtures<sup>7</sup> have provided sufficient background that a working electron impact cross section set for CHF<sub>3</sub> for modeling can be constructed. Morgan has recently discussed compilation of such a cross section set based on swarm measurements and *ab initio* calculations.<sup>8</sup> In this article, the development of a cross section set will be discussed and the derived values will be presented. The cross section set was used in a model of a plasma etching reactor and results for plasma densities will be presented.

## II. DEVELOPMENT OF THE CHF<sub>3</sub> CROSS SECTION SET

The current literature on electron impact interactions with CHF<sub>3</sub> is discussed in detail in Refs. 4, 5, and 7. The highlights from those works, which are of particular interest here, are as follows: (1) There is uncertainty in the magnitude of the cross sections for specific branchings of neutral dissociation. (2) There is a factor of 2 disagreement in total ionization cross section between all measurements and calculations. (3) attachment for electric field/gas number density ( $E/N$ ) < 50 Td (1 Td = 10<sup>-17</sup> V cm<sup>2</sup>) is weak, with some question as to whether measured attachment rates at low  $E/N$  may be a result of impurities. (4) There are relative cross sections available for attachment producing F<sup>-</sup> which indicate a resonance near 10 eV. (5) Measurements for total

scattering are available. (6) Calculated momentum transfer cross sections are available for a limited range of energies.

As a starting point, the neutral dissociation and partial ionization cross sections of Goto *et al.* were used without modification.<sup>9</sup> The cross sections were linearly extrapolated to zero at threshold from the lowest energy cross section available. Dissociative attachment was included using the shape of the F<sup>-</sup> yield as a function of energy measured by Scheunemann *et al.*<sup>10</sup> As a first estimate for the momentum transfer cross section, the total scattering cross section recommended by Christophorou and Olthoff<sup>5</sup> was used at energies below 10 eV, mated to calculations of momentum transfer above 10 eV by Natalense *et al.*<sup>11</sup> Vibrational excitation cross sections were introduced using as threshold energies the values given by Hertzberg for fundamental modes 1-6.<sup>12</sup> Cross sections for nearly degenerate modes were combined yielding three vibrational electron-impact cross sections with thresholds:  $v$ 14, 0.37 eV;  $v$ 25, 0.18 eV, and  $v$ 36, 0.13 eV.

These cross sections were used as input to a solution of Boltzmann's equation for the electron energy distribution using a two-term spherical harmonic expansion.<sup>13</sup> The resulting distributions were then used to compute electron drift velocity and net ionization coefficient [ $\alpha_0 = \alpha - \eta$  where  $\alpha$  is the ionization coefficient (cm<sup>-2</sup>) and  $\eta$  the attachment coefficient (cm<sup>-2</sup>)] as a function of  $E/N$ . Comparisons were made to the experimental swarm measurements of Urquijo *et al.*<sup>6</sup>

Initial trials produced positive values of  $\alpha_0$  many times that of the experiment with the transition from negative to positive  $\alpha_0$  at a lower  $E/N$  than observed experimentally. Additional inelastic or attachment losses were required to bring computed values of  $\alpha_0$  in line with experiment. The magnitudes of the inelastic vibrational cross sections were constrained by the magnitude of the total scattering cross section, and so it was deemed inappropriate to increase their values sufficiently to decrease  $\alpha_0$ . The magnitude of the attachment cross section is likely to be only on the order of 10<sup>-19</sup> cm<sup>24</sup> and is constrained by the small values of experimentally measured  $\eta$  at low  $E/N$ . Therefore, an additional electronic nonionizing inelastic energy loss was required.

<sup>a)</sup>Department of Electrical and Computer Engineering; electronic mail: mjk@uiuc.edu

<sup>b)</sup>Department of Materials Science and Engineering; electronic mail: dzhang@uiuc.edu

This loss was accomplished by increasing the magnitude of the neutral dissociation cross sections since their values are the most uncertain and those reported by Goto are likely too small.<sup>5,14,15</sup> The neutral dissociation cross sections were scaled by values up to 20. Although the appropriate magnitude of  $\alpha_0$  could be obtained, the slope of  $\alpha_0$  versus  $E/N$  could not be matched to swarm data without introducing additional energy loss near threshold. The cross section for the 11.0 eV threshold process ( $e + \text{CHF}_3 \rightarrow \text{CF}_3 + \text{H} + e$ ) was therefore enhanced near threshold. The magnitude of the resonant peak in attachment at 10 eV, the scaling factor for the neutral dissociation cross sections and the magnitude of the enhancement were adjusted so that computed values of  $\alpha_0$  matched the experimental zero crossing of  $\alpha_0$  at  $\approx 65$  Td and the magnitude and slope of  $\alpha_0$  at higher  $E/N$ . The slope of the momentum transfer cross section and the magnitude of the vibrational cross sections were adjusted to match drift velocities. The low energy foot to the attachment cross section was also increased to provide thermal attachment rates of  $3\text{--}4 \times 10^{-14} \text{ cm}^3 \text{ s}^{-1}$ .<sup>7</sup> The cross section for dissociation into CF was arbitrarily partitioned into two equal branchings yielding  $\text{CF} + \text{H} + \text{F}_2$  and  $\text{CF} + \text{H} + 2\text{F}$ , an assumption which has no effect on the computed swarm parameters.

### III. CROSS SECTIONS, SWARM DATA, AND PLASMA PARAMETERS

The resulting cross sections and comparisons of computed swarm data to experiments are shown in Figs. 1–3. Representative electron energy distributions are shown in Fig. 4. Complete tabular data of the cross sections can be obtained by request from the author or can be downloaded from the author's website (<http://uigelz.ece.uiuc.edu/data.html>). The momentum transfer cross section decreases nearly monotonically with energy with a small enhancement near 1 eV in the vicinity of the vibrational cross sections. The nearly flat portion at 2–7 eV was required to lower the drift velocity in the 10s of Td regime while the cross sections from 10–30 eV were constrained by the values from calculations from Natalanse *et al.*<sup>11</sup> The neutral dissociation cross sections were scaled by a factor of 5 from those reported by Goto *et al.*<sup>9</sup> The resulting values are commensurate with measurements by Motlagh and Moore.<sup>15</sup> The enhanced neutral dissociation cross section has a sharply rising leading edge. The calculated swarm parameters are sensitive to this leading edge, however they are not sensitive to the shape of the cross section at energies  $>20$  eV.

In general the agreement of calculated swarm parameters with experimental data is good. The greatest uncertainties are in the drift velocity in the 20–40 Td range and in the attachment coefficient ( $\alpha_0 < 0$ ) in the 40–60 Td range. Larger negative values of  $\alpha_0$  ( $\approx -5 \times 10^{-19} \text{ cm}^2$ ) are computed than indicated experimentally. To eliminate these negative values of  $\alpha_0$  would require that the cross section for attachment at the 10 eV resonant peak be significantly below  $10^{-19} \text{ cm}^2$ . In the absence of this electron attachment, it is difficult to reproduce the zero crossing in  $\alpha_0$ . Increasing the foot in the attachment cross section produces too much attachment at low  $E/N$  at electron energies below 1.8 eV where attachment rates are small if they exist at all.

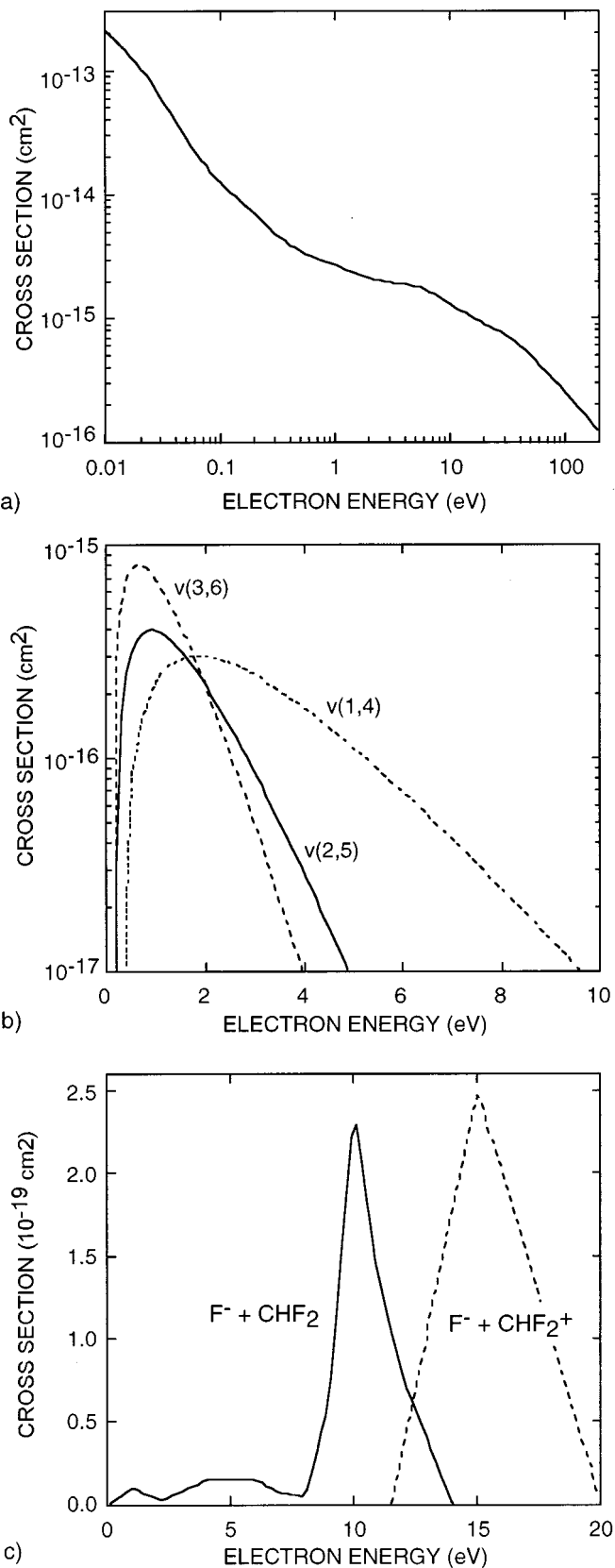


FIG. 1. Derived electron impact cross sections for CHF<sub>3</sub>. (a) Momentum transfer, (b) vibrational excitation, and (c) attachment.

Representative electron energy distributions (EEDs) are shown in Fig. 4 for swarms in pure CHF<sub>3</sub>. The EEDs for  $E/N < 60$  Td are shaped by inelastic energy loss through vibrational excitation. At lower  $E/N$ , this loss is dominated by

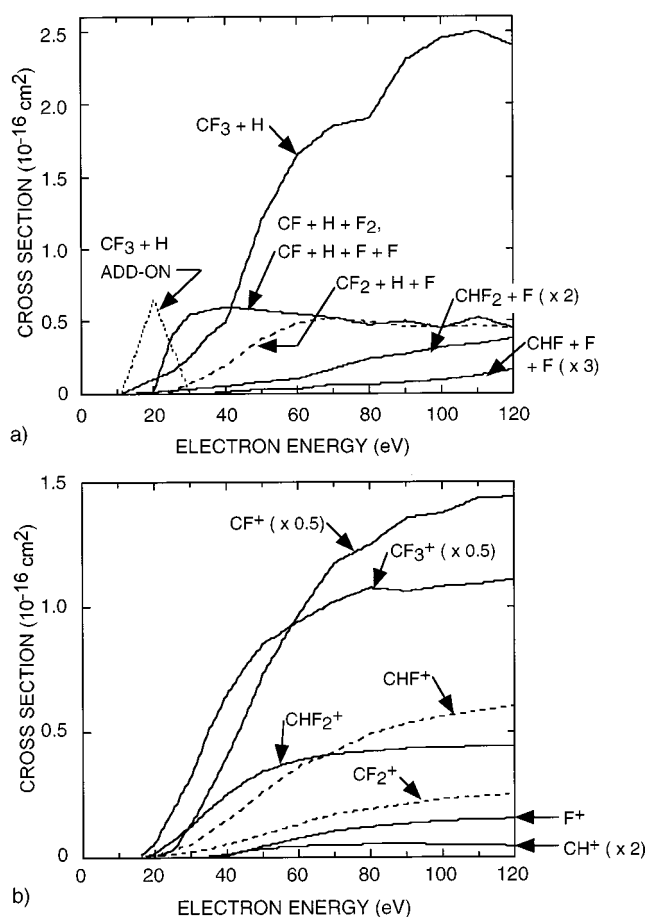


FIG. 2. Derived electron impact cross sections for CHF<sub>3</sub>. (a) Neutral dissociation and (b) ionization and electronic excitation. The neutral dissociation cross sections from Goto (Ref. 9) were increased by a factor of 5, and a threshold enhancement was added. The ionization cross sections from Goto were used without change.

*v*3,6. At the higher *E/N*, contributions from *v*2,5 begin to become important. At *E/N* = 80 Td, energy loss from the enhanced 11.0 eV neutral dissociation process accounts for about 3% of the energy loss, and the lowest threshold ionization process (15.2 eV) accounts for about 0.1%. These fractions increase to 15% and 1% at 100 Td and are responsible for the cutoff of the EED. The electron temperature ( $T_e = 2/3\langle \epsilon \rangle$ ), shown in Fig. 3(a), increases rapidly from 0.1 to 2–3 eV for *E/N* < 100 Td. At *E/N* > 100 Td, the larger rates of power loss to dissociation and ionization results in the electron temperature saturating in the 4–5 eV range

Using this cross section set, simulations were performed of a low pressure inductively coupled plasma reactor of the type used for plasma etching. The model used is the Hybrid Plasma Equipment Model, described in detail in Ref. 16. A schematic of the reactor is in Ref. 17. The operating conditions are 10 mTorr, 300 sccm, and power deposition of 200–650 W, values that were chosen to minimize the fractional dissociation. The reactor volume averaged electron and negative ion densities as a function of power for CHF<sub>3</sub> and C<sub>2</sub>F<sub>6</sub> at the same conditions are shown in Fig. 5. In both cases, the reactor averaged electron densities scale nearly linearly with power and are 1–5 × 10<sup>10</sup> cm<sup>-3</sup>. The electron

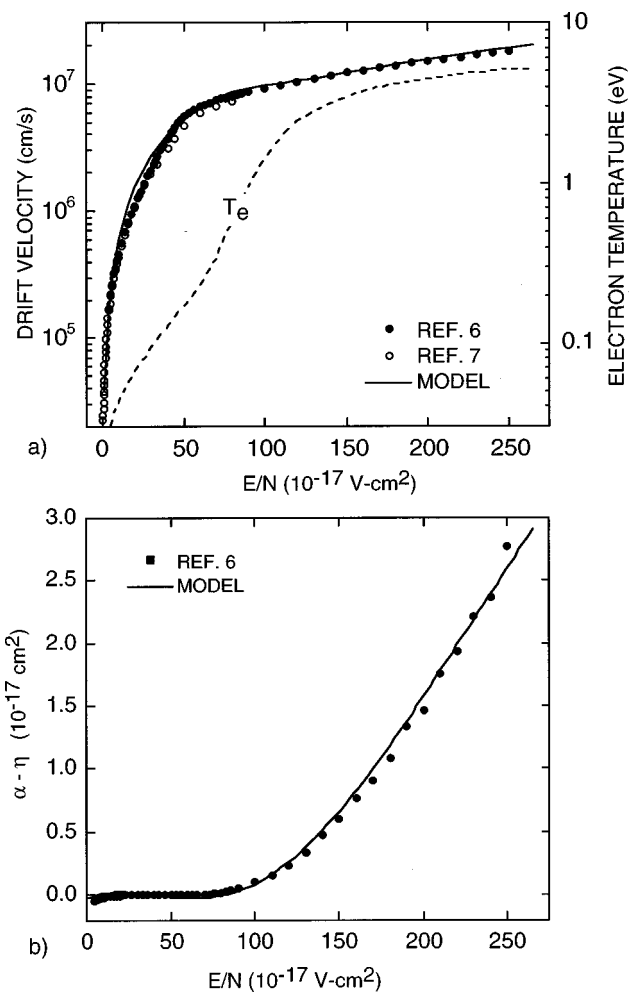


FIG. 3. Electron swarm data for CHF<sub>3</sub>. (a) Drift velocity and electron temperature and (b) net ionization coefficient. Agreement of calculated swarm parameters with experiment is generally good, with some overestimation of the drift velocity in the 20–40 Td range.

energy loss processes for the two molecules are commensurate and so for a given power deposition, the electron densities will be approximately the same, although the electron density for CHF<sub>3</sub> is systematically generally larger than for

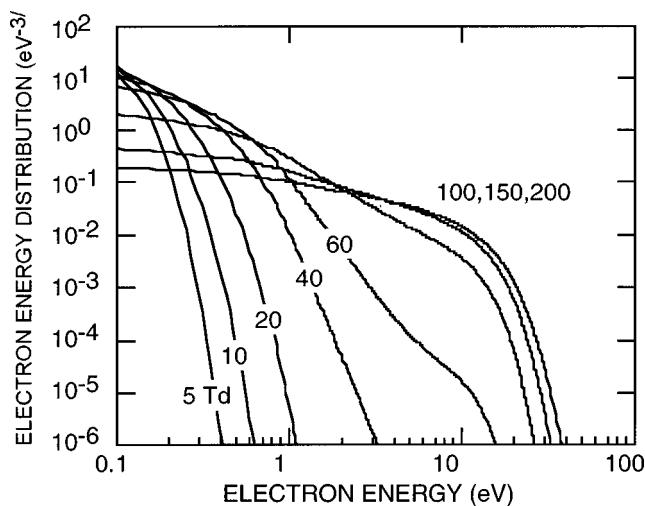


FIG. 4. Representative electron energy distributions for swarms in CHF<sub>3</sub> for *E/N* of 5–200 Td.

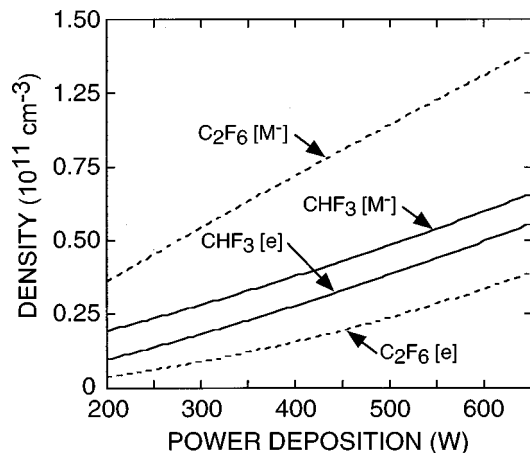


FIG. 5. Reactor averaged electron and negative ion densities for inductively coupled plasmas at 10 mTorr in  $\text{CHF}_3$  and  $\text{C}_2\text{F}_6$ .

$\text{C}_2\text{F}_6$ . The attachment cross sections for  $\text{C}_2\text{F}_6$ , though not large, are larger than for  $\text{CHF}_3$ . This results in a higher rate of attachment and a larger negative ion density for  $\text{C}_2\text{F}_6$  compared to  $\text{CHF}_3$ . These trends agree with measurements of electron density and negative ion density by Hebner and Miller<sup>18</sup> in inductively coupled plasmas for similar conditions.

#### IV. CONCLUDING REMARKS

A working cross section set for  $\text{CHF}_3$  has been presented and favorably compared to swarm data. Uncertainties in measurements of attachment rates at low  $E/N$  have resulted in some uncertainty in the derived attachment cross section. An enhanced dissociation cross section near threshold was used to match the slope of the ionization coefficient to swarm data. Using these cross sections in a plasma equipment model, we found that negative ion densities are generally higher in  $\text{C}_2\text{F}_6$  compared to  $\text{CHF}_3$ .

#### ACKNOWLEDGMENTS

This work was supported by the National Science Foundation (CTS 99-74962), the Semiconductor Research Corporation, and AFOSR/DARPA. The authors thank Professor Urquijo for access to his swarm data prior to publication.

- <sup>1</sup>N. R. Rueger, J. J. Beulens, M. Schaepekens, M. F. Doemling, J. M. Mirza, T. E. F. M. Standearts, and G. S. Oehrlein, *J. Vac. Sci. Technol. A* **15**, 1881 (1997).
- <sup>2</sup>R. P. Jayaraman, R. T. McGrath, and G. A. Hebner, *J. Vac. Sci. Technol. A* **17**, 1545 (1999).
- <sup>3</sup>K. Takahashi, M. Hori, and T. Goto, *Jpn. J. Appl. Phys., Part 1* **33**, 4745 (1994).
- <sup>4</sup>L. G. Christophorou, J. K. Olthoff, and M. V. V. S. Rao, *J. Phys. Chem. Ref. Data* **26**, 1 (1997).
- <sup>5</sup>L. G. Christophorou and J. K. Olthoff, *J. Phys. Chem. Ref. Data* **28**, 967 (1999).
- <sup>6</sup>J. de Urquijo, I. Alvarez, and C. Cisneros, *Phys. Rev. E* **60**, 4990 (1999).
- <sup>7</sup>Y. Wang, L. G. Christophorou, J. K. Olthoff, and J. K. Verbrugge, *Chem. Phys. Lett.* **304**, 303 (1999).
- <sup>8</sup>W. L. Morgan, 52nd Gaseous Electronics Conference, Norfolk, VA, October 1999.
- <sup>9</sup>M. Goto, K. Nakamura, H. Toyoda, and H. Sugai, *Jpn. J. Appl. Phys., Part 1* **33**, 3602 (1994).
- <sup>10</sup>H.-U. Scheuenemann, M. Heni, E. Illenberger, and H. Baumgartel, *Ber. Bunsenges. Phys. Chem.* **86**, 321 (1982).
- <sup>11</sup>A. P. P. Natalense, M. H. F. Bettega, L. G. Ferreira, and M. A. P. Lima, *Phys. Rev. A* **59**, 879 (1999).
- <sup>12</sup>G. Herzberg, *Molecular Spectra and Molecular Structure, II. Infrared and Raman Spectra of Polyatomic Molecules* (Van Nostrand, New York, 1945).
- <sup>13</sup>S. D. Rockwood, *Phys. Rev. A* **8**, 2348 (1973).
- <sup>14</sup>H. Sugai, H. Toyoda, T. Nakano, and M. Goto, *Contrib. Plasma Phys.* **35**, 415 (1995).
- <sup>15</sup>S. Motlagh and J. H. Moore, *J. Chem. Phys.* **109**, 432 (1998).
- <sup>16</sup>S. Rauf and M. J. Kushner, *J. Appl. Phys.* **83**, 5087 (1998).
- <sup>17</sup>D. Zhang and M. J. Kushner, *J. Appl. Phys.* **87**, 1060 (2000).
- <sup>18</sup>G. A. Hebner and P. A. Miller, *J. Appl. Phys.* **87**, 7660 (2000).